

Comparison of the Biological Damage Produced by Somatostatin Analog Radiopharmaceuticals Labelled with ^{161}Tb and ^{177}Lu

L. Meléndez-Alafort^{1,2}, E. Azorín-Vega³, G. Ferro-Flores³, C. Bolzati^{4,5}, E. Farinelli⁶, M. Bello^{2,6}, A. Rosato^{1,7}, L. De Nardo^{5,6}.

¹ Veneto Institute of Oncology IOV-IRCCS, Padova, Italy. ² INFN, Laboratori Nazionali di Legnaro, Legnaro (Padova), Italy

³ Department of Radioactive Materials, Instituto Nacional de Investigaciones Nucleares, Ocoyoacac, Mexico. ⁴ Institute of Condensed Matter Chemistry and Energy Technologies ICMATE-CNR, Padova, Italy. ⁵ INFN, Sezione di Padova, Padova, Italy.

⁶ Department of Physics and Astronomy, University of Padova, Padova, Italy. ⁷ Department of Surgery, Oncology and Gastroenterology, University of Padova, Padova, Italy.

INTRODUCTION

Targeted radionuclide therapy (TRT) is a nuclear medicine technique based on the use of radiopharmaceuticals (RPs) with high affinity to antigens present on the surface of tumour cells, which allows the systemic radiation treatment of tumours and their metastatic lesions with minimal dose to normal tissues [1]. ^{177}Lu -RPs are currently the most used for TRT because they have demonstrated a favourable safety and good response rates to treatment. However, the number of commercial suppliers of the ^{177}Lu non-carrier added required for the TRT is limited, so its worldwide availability may not be sufficient in the long term [2]. To solve this problem, Lehenberger *et al.* proposed using ^{161}Tb for TRT because its chemical and decay properties are similar to those of ^{177}Lu [3] (see Table 1). Moreover, it has been found that ^{161}Tb -RPs enhance the therapeutic efficacy of ^{177}Lu -RPs since ^{161}Tb emits a significantly higher amount of internal conversion electrons (IE) and Auger electrons (AE) of energies ≤ 40 keV, which increase the absorbed dose by the cells [4].

Recently Borgna *et al.* labelled three somatostatin analogues (SST) (DOTATOC-NLS, DOTATOC, and DOTA-LM3) with ^{161}Tb and ^{177}Lu to study the effect of the RPs localization on AR42J cell viability and survival and concluded that IE and AE emitted by ^{161}Tb contributed positively to its therapeutic efficacy [5]. However, the authors did not perform dosimetric studies.

This study aimed to assess and compare the biological damage produced by ^{161}Tb -SST and ^{177}Lu -SST RPs localized in different regions within AR42J cells through cellular dosimetry and cell survival fraction assessment using the MIRDcell code [6,7].

Table 1. Comparison of ^{177}Lu and ^{161}Tb main decay characteristics.

	γ -emission		β -emission		IE keV/decay	AE keV/decay	Total electron energy/decay (keV)
	E_γ (keV)	I_γ (%)	$E_{\beta\text{-avg}}$ (keV)	I_β (%)			
^{177}Lu $T_{1/2} = 6.64$ d	112 208	6 11	47 111 149	12 9 79	13.5	1.13	147.9
^{161}Tb $T_{1/2} = 6.89$ d	26 46* 49 75	23 11 17 10	138 157 175 184	25 65 5 5	39.2	8.94	202.5

*x-ray

METHODS

Fluorescence images of alginate-embedded AR42J cells co-stained with propidium iodide ($1\mu\text{M}$) and calcein green AM ($1\mu\text{M}$) were acquired with an inverted microscope ImageXpress XL (Molecular Devices). Obtained images were analysed with Metaxpress software to determine the mean area of cells and nuclei of 50 cells.

Absorbed dose (AD) in AR42J cells after incubation with one of the SST analogues (DOTATOC-NLS, DOTATOC, or DOTA-LM3) labelled with ^{161}Tb or ^{177}Lu were assessed with MIRDcell Software using as program input the full data electron emissions (β -spectra, IC, and AE) of each radionuclide obtained from the International Commission on Radiological Protection publication ICRP-107 [8].

The mean AD in the cell nucleus per unit of cumulated activity (S-Values) was obtained for each labelled-SST analogue, considering the membrane, cytoplasm, or nucleus as source regions (where the radioactivity was evenly distributed) and the cell nucleus as the only target region. Then, total AD in the cell nucleus per unit of cumulated activity was calculated for each RPs using the obtained S-values and the reported percentage of activity of ^{161}Tb -SST or ^{177}Lu -SST analogues in the cell source regions [5] (see Table 2), using the following equation:

$$AD_{(\text{target} \leftarrow \text{source})} = N_{(\text{source})} \times S_{(\text{target} \leftarrow \text{source})} \quad (1)$$

where $N_{(\text{source})}$ is the number of disintegrations in the source region per unit of administered activity (Bq·h/Bq).

Table 2. Uptake and distribution of radiolabelled-somatostatin analogue in AR42J cells.

SST analogue	Total uptake	Source region		
		Membrane	Cytoplasm	Nucleus
DOTATOC	10 %	19 %	80 %	1 %
DOTATOC-NLS	15 %	16 %	78 %	6 %
DOTA-LM3	70 %	92 %	7 %	2 %

Finally, MIRDcell software was used to estimate the survival fraction of a 3D multicellular cluster of different sizes with a spherical shape after the treatment with one of ^{161}Tb -SST or ^{177}Lu -SST RPs, using as a percentage of labelled cells the total uptake reported in Table 2. The cell survival probability (P) was obtained using the linear quadratic model equation 2, which takes into account the AD

generated by the radiation emitted within the same cell (self) and the radiation emitted by neighbouring cells (cross) [9].

$$P = e^{-\alpha_{self}D_{self} - \beta_{self}D_{self}^2} \times e^{-\alpha_{cross}D_{cross} - \beta_{cross}D_{cross}^2} \quad (2)$$

where the α and β values of PC3 cells (0.551 and 0.21, respectively) were used because they present similar radioresistance to AR42J cells.

RESULTS

The mean diameter of the AR42J cell and its nucleus obtained by microscopic measurements of cell imaging was $8 \pm 1 \mu\text{m}$ and $6 \pm 1 \mu\text{m}$, respectively (see Fig. 1).

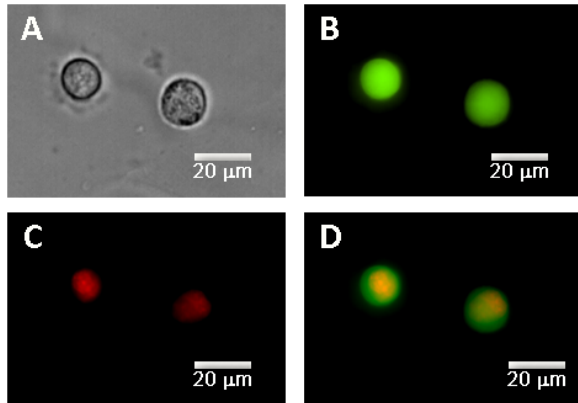


Fig. 1. Representative image of alginate-embedded AR42J cells: A) phase contrast image, B) cytoplasmic distribution of calcein (green) in alive cells, C) nuclear imaging, staining with propidium iodide (red), and D) combined images of B) and C).

Dosimetric studies show that ^{161}Tb labelled RPs produced much higher nucleus AD than those labelled with ^{177}Lu . In all the cases, the higher average nucleus AD was obtained with a larger cell cluster, where cells absorbed a greater percentage of the energy emitted by the radionuclide (see Fig. 2). The ^{177}Lu -RPs localization within the cells does not significantly affect the produced nucleus AD. In contrast, small differences in AD were found after ^{161}Tb -RPs treatment.

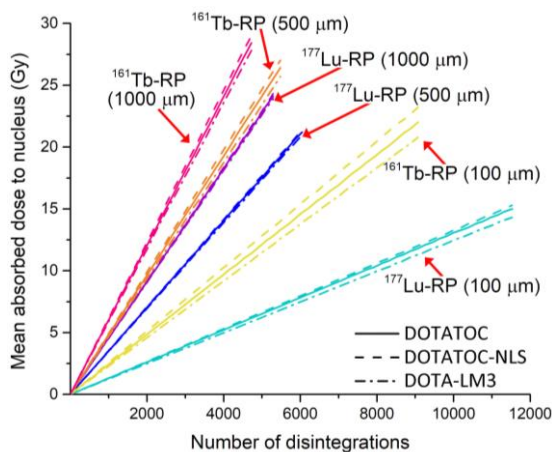


Fig. 2. Mean nucleus absorbed doses obtained after treatment of three cell clusters of different sizes with ^{161}Tb -RPs and ^{177}Lu -RPs.

DOTATOC-NLS produces the highest AD due to its higher concentration in the nucleus, followed by DOTATOC and DOTA-LM3, which were mainly localized in the cytoplasm and the cell membrane respectively. However, the factor that has the greatest influence on the cell survival was the RPs total uptake. Using equal number of disintegrations, the treatment with DOTA-LM3 resulted in the lower cell survival fraction (SF), despite this agent produces the lower nucleus AD (see Fig. 3).

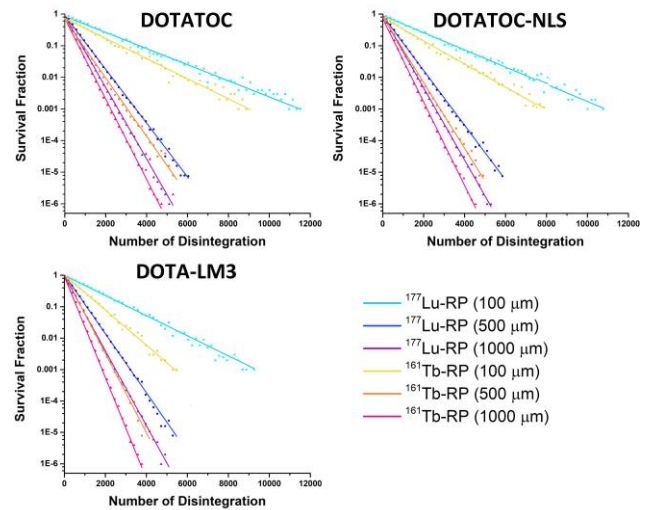


Fig. 3. Comparison of the AR42J cells SF after the treatment with ^{161}Tb -RPs and ^{177}Lu -RPs.

CONCLUSIONS

Dosimetry evaluations conducted in this study reveal that most of the β -particles emitted by ^{177}Lu penetrate from the membrane to the nucleus. Therefore, the cellular localization of ^{177}Lu -RPs does not affect the nucleus AD and the generated biological damage. In contrast, ^{161}Tb -RPs localization in small cluster causes differences in the nucleus AD due to the IE and AE emitted by ^{161}Tb . However, when the cluster size increases, the AD difference due to the RPs localization is minimal and the survival fraction depends mainly on the RPs total uptake.

^{161}Tb -RPs produce higher biological damage than ^{177}Lu -RPs with the same number of disintegrations.

- [1] J. Malcolm, et al., *Cancers*. 11 (2019) 12.
- [2] W. V. Vogel, et al., *Eur. J. Nucl. Med. Mol. Imaging*. 48 (2021) 2329.
- [3] S. Lehenberger, et al., *Nucl. Med. Biol.* 38 (2011) 917.
- [4] C. Muller, et al., *Eur. J. Nucl. Med. Mol. Imaging*. 46 (2019) 1919.
- [5] F. Borgna, et al., *Eur. J. Nucl. Med. Mol. Imaging*. 49 (2022) 1113.
- [6] S. Katugampola, et al., *J. Nucl. Med.*. 63 (2022) 1441.
- [7] B. Vaziri, et al., *J. Nucl. Med.*. 55 (2014) 1557.
- [8] ICRP-2008, *Ann. ICRP* 32 (2008).
- [9] L. De Nardo, et al., *Medical Physics*. 49 (2022) 2709.